Scripta Materialia 130 (2017) 187–190

Contents lists available at ScienceDirect

Scripta Materialia

journal homepage: www.elsevier.com/locate/scriptamat

Regular Article

A comparison of power controlled flash sintering and conventional sintering of strontium titanate

Fabian Lemke, Wolfgang Rheinheimer *, Michael J. Hoffmann

Institute of Applied Materials - Ceramic Materials and Technologies, Karlsruhe Institute of Technology (KIT), Haid-und-Neu-Str. 7, 76131 Karlsruhe, Germany

ARTICLE INFO

Article history:
Received 1 December 2016
Received in revised form 7 December 2016
Accepted 7 December 2016
Available online xxxx

Keywords:
Flash sintering
Electric field assisted sintering
Strontium titanate
Joule heating

ABSTRACT

The microstructural evolution of $SrTiO_3$ is analyzed during power controlled flash sintering. A controllable sintering process is achieved by lowering the specific power densities yielding a relatively slow flash sintering. The analytical equations for sintering developed by Coble are used to characterize flash sintering. The focus is on the evolution of microstructure with time and its comparison with conventional sintering. The results are discussed in comparison to the active sintering mechanism, the impact of joule heating and to the current state of research on flash sintering of ZrO_2.

Since the first appearance of flash sintering, ZrO_2 was used as a model material to understand the acceleration of sintering in electric fields and with electric currents [1–7]. Aspects like joule heating, a change of the defect chemistry and structural lattice changes are considered to cause the fast densification of zirconia [8–10]. Nevertheless flash sintering is not yet fully understood for zirconia; for other material classes even less information is available. For perovskites such as $SrTiO_3$ a change of the defect chemistry or of the crystal structure seems not to occur [11].

Apparently joule heating is of significant impact during flash sintering of all materials. Its impact on the sample temperature during flash sintering was investigated in vast detail and is generally well understood [9,12], although there may be effects due to local overheating at particle necks and, thus, internal temperature distribution in the sample. The sample temperature T_{calc} during flash sintering was obtained under consideration of the black body radiation [9]

$$\frac{T_{calc}}{T_{meas}} = \left[1 + \frac{1000 \cdot W_V}{\sigma \cdot T_{meas}^4} \cdot \left(\frac{V}{A}\right)\right]^{1/4} \quad (1)$$

with the measured sample temperature T_{meas}, the volumetric power dissipation of the sample W_V, the volume to area ratio V/A and a universal physical constant $\sigma = 5.67 \cdot 10^{-8} Wm^2K^{-4}$.

The microstructural evolution during flash sintering is hard to observe since densification is very fast and quenching from a setup with electric contacts is experimentally difficult. In this study we present a method where the samples undergo a relatively slow flash sintering process with low current and power densities. By limiting the power source output, densification remains controllable and proceeds within a few minutes. The densification process is analyzed analogue to conventional sintering using the well-known Coble model [13–15]. A simplified equation for the densification rate $\dot{\rho}$ is given by

$$\dot{\rho} = C \cdot D/G^m \quad (2)$$

where C is a constant, D is the diffusion coefficient and G is the mean grain diameter. The exponent m depends on the dominating diffusion mechanism ($m = 3$ for volume diffusion and $m = 4$ for grain boundary diffusion).

High purity strontium titanate powder was prepared by the mixed oxide/carbonate route using $SrCO_3$ and TiO_2 (purities of 99.95 and 99.995%, respectively, Sigma Aldrich Chemie GmbH, Taufkirchen, Germany). The Sr/Ti ratio was 0.996. Cylindrical green bodies were uniaxially pressed (6 mm long and 8 mm in diameter) in a steel die and subsequently cold-isostatically pressed at 400 MPa. Geometric green densities were found to be 63 ± 1%.

Flash sintering experiments were conducted in an optical dilatometer (TOMMI plus, Fraunhofer ISC, Germany). Samples were contacted with platinum wire spirals as electrodes and platinum wires as cables. The furnace was heated to 1120 °C or 1150 °C. After 10 min of equilibration time an electrical field was applied to the samples (XG 600-2.8, Ametek, United States). The field was limited to 500 V/cm, but for all experiments reported here this field was reached only initially, since the

* Corresponding author.
E-mail addresses: Fabian.Lemke@kit.edu (F. Lemke), Wolfgang.Rheinheimer@kit.edu (W. Rheinheimer), michael.hoffmann@kit.edu (M.J. Hoffmann).

http://dx.doi.org/10.1016/j.scriptamat.2016.12.008
1359-6462/

high conductivity of the samples resulted in current-controlled output. The current limit I_{max} was varied to limit and control the power dissipation of the sample. The power density is assumed to be

$$P_V = \frac{U \cdot I}{V} \quad (3)$$

with the voltage U applied to the sample, the current I flowing through the sample and the sample volume V. As will be shown later, the powder dissipation reached a steady state within short times. In the present experiments the maximum power density was ~100 mW/mm^2.

Sintered samples were prepared for SEM imaging to observe microstructures. Polished samples were thermally etched at 1075 °C for 2 h. The average grain size was obtained by the line intersection method observing more than 500 grains per sample (AnalySis Software, Olympus, Japan).

Table 1 gives the furnace and power source conditions as well as the measured and estimated true sample temperature. The measured sample temperature refers to a thermocouple close to the sample. A comparison of the furnace temperature $T_{furnace}$ and the measured sample temperature T_{meas} shows that increasing current limits result in significant joule heating of the sample. However, T_{meas} cannot give the true temperature of a sample that is heated by joule heating. Thus Eq. (1) was used to estimate the true sample temperature T_{calc} needed for a comparison with conventional sintering. Accordingly the temperature increase by joule heating is $\Delta T = T_{calc} - T_{furnace}$.

For a set of isothermal experiments (1150 °C, I_{max} = 100 mA to 500 mA) the power density and the shrinkage L/L_0 are shown in Fig. 1. As the field is applied, the high conductivity of the material results in current controlled output within a few minutes. At a furnace temperature of 1150 °C, the power density reaches a steady state for I_{max} = 100 mA. For 200 mA, the power density almost reaches a steady state as well, but with significant instability (i.e. scattering and slight increase with time). However, for 500 mA a very unstable powder density is evident: strong scattering occurs along with a significant increase with time.

The linear shrinkage strongly depends on the power density. For 500 mA the sample densifies within 5 min. However, after densification the sample slightly elongates with time. A comparison with the power density (which also increases with time) suggests that the sample temperature increases and thermal expansion occurs. For 100 mA and 200 mA, densification is slower and very similar to conventional sintering behavior [16].

Since a comparison of field assisted sintering and conventional sintering requires stable experimental conditions (i.e. constant power dissipation at the sample), the furnace temperature was decreased and the current limit increased to find a set of parameters, which results in stable power dissipation but with significant joule heating. At a furnace temperature of 1120 °C and a current limit of 120 mA, very stable power dissipation was reached with an estimated sample temperature of 1240 °C (cf. Fig. 1 and Table 1). The resulting field at the sample was ~80 V/mm. This dataset was chosen for a detailed comparison to conventional field-free sintering at 1280 °C [16].

The densification for conventional sintering at 1280 °C and for field assisted sintering at T_{calc} = 1240 °C (I_{max} = 120 mA) is shown in Fig. 2a. For both experiments several curves are shown indicating

Table 1
Current limit, furnace temperature, measured and calculated sample temperature and estimated temperature increase of the sample by joule heating (see text for details).

$T_{furnace}$	I_{max}	T_{meas}	T_{calc}	ΔT
1120 °C	120 mA	1170 °C	1240 °C	120 °C
1150 °C	100 mA	1180 °C	1190 °C	40 °C
1150 °C	200 mA	1190 °C	1275 °C	125 °C
1150 °C	500 mA	1200 °C	1345 °C	195 °C

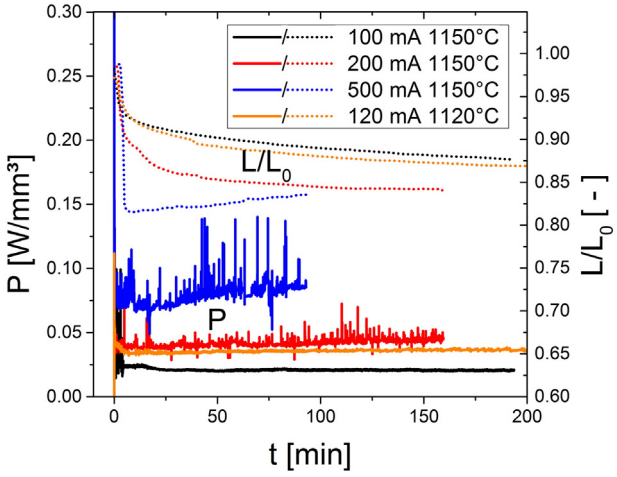

Fig. 1. Power densities and linear shrinkage during power controlled flash sintering for three different current limits. The furnace temperature was 1150 °C for 100 mA, 200 mA and 500 mA and 1120 °C for 120 mA.

different heating times. In general, both experimental setups show very similar densification. For field assisted sintering the densification is slightly slower than for conventional sintering, but given the estimated temperature difference of 40 K this is to be expected (conventional sintering at 1280 °C and field assisted sintering at 1240 °C).

For both setups the mean grain size was measured after different heating times (cf. Fig. 2b). Again both setups give very similar results with the field assisted sintering having slightly smaller grain sizes, most likely for the same reason as the slower densification. Fig. 3 shows microstructures after 30 min and 120 min for field assisted and conventionally sintered samples. Besides minor differences in porosity

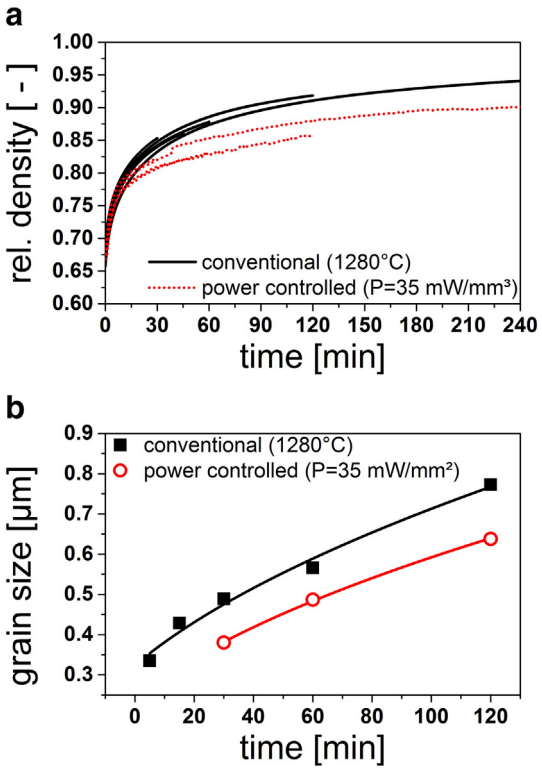

Fig. 2. Relative density of power controlled flash sintering with 35 mW/mm^3 at a furnace temperature of 1120 °C compared to conventional sintering at 1180 °C (a). Evolution of the grain size during sintering for power controlled flash sintering and conventional sintering at 1180 °C (b).